Spectroscopic Studies of Hexadecylquinolinium Tricyanoquinodimethanide

Jeffrey W. Baldwin, Bo Chen, Shane C. Street, Valery V. Konovalov, Hiromi Sakurai,† Terry V. Hughes, Camino S. Simpson,‡ M. V. Lakshmikantham, Michael P. Cava, Lowell D. Kispert, and Robert M. Metzger*

Laboratory for Molecular Electronics, Chemistry Department, University of Alabama, Tuscaloosa, Alabama 35487-0336

Received: September 17, 1998; In Final Form: January 28, 1999

Hexadecylquinolinium tricyanoquinodimethanide (**1**), a unimolecular rectifier of electrical current with a large ground-state dipole moment (43 ± 8 D), reveals large hypsochromic shifts of the absorption spectrum. Two fluorescent emissions were observed: one in the visible region (quantum yield $\phi \approx 0.01$, not solvatochromic) and one in the near-infrared spectrum (weakly solvatochromic). Using a prolate spheroidal cavity model and the absorption maxima measured in eight solvents, the excited-state dipole moment of **1** is estimated as 8.7 D. The NMR spectral lines broaden above 330 K and lose the multiplet structure. The core-level N 1s XPS spectrum reveals the three expected N valence states. The valence-level XPS spectrum can be correlated with theory. Simultaneous cyclic voltammetry and electron spin resonance of the radical anion of **1** shows that the spin density in the LUMO of **1** is concentrated on the tricyanoquinodimethanide portion of the anion. The molecule is clearly zwitterionic in the ground state, both in LB films and in solution, and is undissociated ("neutral") in its first excited state.

1. Introduction

Unimolecular electrical rectification, i.e., asymmetric electrical conduction, was recently demonstrated[1] through a single molecule of hexadecylquinolinium tricyanoquinodimethanide, $C_{16}H_{33}Q-3CNQ$ (**1**) by a modification of the Aviram−Ratner mechanism.[2]

Several issues deserve, and receive here, further attention. It was suggested that **1** may belong to a class of twisted internal charge transfer molecules.[3] The solvatochromism[1] of the absorption spectrum of **1** is used to estimate the excited-state dipole moment. We also report here fluorescence emission spectra for **1**. The spin distribution of the radical anion of **1** was measured by electron spin resonance. Finally, the X-ray core-level and valence-band photoelectron spectra of **1** gives information about the nature (zwitterionic or undissociated) of the ground state and about the valence-level molecular orbitals.

2. Ground and Excited States of 1

Ashwell and co-workers discovered a new class of zwitterions; a quaternary picolinium or lepidinium halide, when reacted with an alkali salt of TCNQ, can yield, instead of a charge-transfer ion-radical salt, a covalently bonded zwitterionic adduct, with loss of HCN.[4] Similar chemical reactions occur with quaternary ammonium compounds and tetracyanoethylene.[6,7] The first such molecule was picolyl tricyanoquinodimethane, or picolinium tricyanoquinodimethanide, P-3CNQ, **2**; its crystal structure is that of a ground-state zwitterion, with a $\theta = 30°$ twist[4] between the pyridinium ring and the central six-membered ring of $3CNQ^-$ and a ground-state calculated dipole moment of 26 D.[4] The optical spectrum of a crystal of **2** shows two bands: an intramolecular absorption (intervalence transfer, or IVT) at 18 600 cm^{-1}, and an intermolecular absorption (or intermolecular charge transfer, or ICT) at 12 400 cm^{-1}.[8]

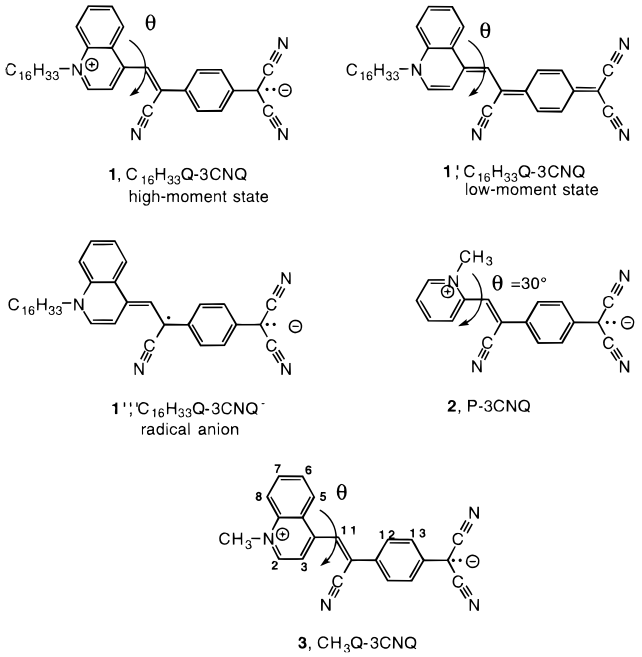

These molecules, when made suitably amphiphilic by addition of long alkyl terminations, yield Z-type Langmuir−Blodgett films with high second-order nonlinear optical coefficients $\chi^{(2)}$;[5] they exhibit a narrow and solvatochromic absorption band.[5]

The most interesting member of this class is $C_{16}H_{33}Q-3CNQ$ (**1**), which is blue in acetonitrile solution.[9] That **1** may be a zwitterion is made obvious by depicting it as a $D^+-\pi-A^-$ molecule, where D^+ is the hexadecylquinolinium moiety, π is the two-carbon π-electron bridge, and A^- is the tricyanoquino-

* To whom correspondence should be sent.

† Present Address: Department of Applied Chemistry, University of Tokyo, Komaba, Tokyo, Japan.

‡ Present Address: Talladega College, Talladega, AL 35160.

10.1021/jp983759u CCC: $18.00
Published on Web 04/30/1999

dimethanide ($3CNQ^-$) moiety. The blue color, which is strongly solvatochromic, was assigned to an IVT band.[1]

No crystal structure could be determined for **1**; only small multiply twinned crystallites were obtained.[1] Therefore, the twist angle θ between the quinolinium ring and the ethylene bridge (shown in the diagram above) is not known experimentally.[1] If $\theta = 0°$, then **1** could be construed either as a zwitterionic molecule $D^+-\pi-A^-$ or as an undissociated ("neutral") molecule $D^0-\pi-A^0$; these two states would be resonance forms with no independent existence. If $\theta = 90°$, then **1** must perforce be a zwitterion, i.e., **1** would have a twisted internal charge transfer (TICT) state[3] with no intramolecular intervalence (IVT = 0) band possible; in this state, the molecule should be colorless. The steric hindrance between the central cyano group nitrogen atom and the hydrogen atoms on the quinolium ring probably hinders free molecular rotation and causes θ to remain considerably larger than 0°. In the ground state, if **1** is zwitterionic ($D^+-\pi-A^-$), then θ is probably intermediate between 0° and 90°. The angle θ may change during electronic excitation.

Semiempirical molecular orbital calculations (using, in particular, the AM1 or PM3 algorithms) suggest that in the "gas phase" **1** in the ground state should have $\theta = 9°-11°$,[3] with dipole moments of the order of 10 D, while in the first excited state $\theta \approx 90°$,[3] with dipole moments of the order of 45 D. If one adds a "solvent" to the algorithm,[10] then high dipole moments are calculated (40−50 D), both for the ground state and for the first excited state.[3] It was suggested that **1** is zwitterionic in solution but undissociated in films.[11,12]

The long-wavelength absorption maximum in the visible region of **1** is solvent-dependent, i.e., negatively solvatochromic, or hypsochromic; this maximum was at 720 nm in CH_3CN (blue solution[9]), at 884 nm in CH_2Cl_2, and at 838 nm in $CHCl_3$.[1] For CH_3CN and CH_2Cl_2 the absorbance was linear with concentration, while in $CHCl_3$ there was a small deviation from linearity.[1] In LB films, the blue color is due to a narrow absorption band, with a maximum at 565 nm[9] or 570 nm[1] and a half-width at a half-maximum of 22 nm.[9]

In acidic CH_3CN the blue color of **1** disappears ("bleaches")[13] when the molecule protonates at the $C(CN)_2$ end;[1] the resulting protonated anion is colorless. When the protonated anion is exposed to ammonia, the blue color returns.[1] In $CHCl_3$ solution, a phosgene impurity can form photochemically; in the presence of water, phosgene produces HCl, which can then protonate **1**. Samples of **1**, sealed in a N_2 atmosphere and stored in a refrigerator over a long period of time, can exhibit less of the blue color when first dissolved. With time, the blue color becomes more intense.[14]

1 forms Z-type Langmuir−Blodgett multilayers with a very high second-order nonlinear optical susceptibility $\chi^{(2)}_{zzz} = 180$ pm V^{-1}.[15] Using solutions of **1** in CH_2Cl_2, we measured a dipole moment of 43 ± 8 D for **1** at infinite dilution.[1] The blue narrow absorption band in solution was assigned to IVT; when several molecules are packed in a multilayer, an ICT may occur, as it does for **2**, but for **1** an ICT has not been reported.

It is believed[5,9,16] that the ground state of **1** is very polar, while its first excited state is less polar, of the type $D^0-\pi-A^0$ (**1′**), and that the efficiency for frequency doubling is due to the zwitterion−undissociated molecule transition:

$$D^+-\pi-A^- \rightarrow D^0-\pi-A^0$$

Electrical rectification was seen for Langmuir−Blodgett (LB) multilayers of **1** sandwiched between dissimilar metal electrodes.[5,16] The work was repeated,[1] extended securely to a monolayer of **1**,[1] using the same metal (Al) on the two sides of the Langmuir−Blodgett monolayer[1] and also a STM Pt/Ir probe atop the LB monolayer of **1** on graphite.[1] **1** is a unimolecular rectifier of electrical current. The measured direction of rectification for **1** assumes that the ground state is a zwitterion and that the electrically accessed excited state has a lower dipole moment than the ground state does. The contradictory results from theoretical calculations require, therefore, that the change in dipole moment be better understood.

We present here new spectroscopic results for molecule **1**. We were interested in probing how possible changes in the twist angle θ may affect the mixing or interaction between a low-moment state (**1′**) and the high-moment state (**1**). We probed its photochromism in solution to estimate its excited-state dipole moment and its fluorescence. We measured the temperature-dependent nuclear magnetic resonance (NMR) spectrum of the methyl analogue of **1** namely molecule **4**, to get more information about its ground-state conformation. We studied the XPS spectrum of an LB monolayer and multilayer of **1** to observe the number of chemically unique N atoms in the molecule. We obtained the electron paramagnetic resonance (EPR) spectrum of its radical anion **1‴** at its reversible electrochemical reduction wave, to see on which end of **1‴** the spin densities are concentrated.

3. Instrumentation

Visible−UV spectra were measured on a Shimadzu UV-1600 spectrophotometer. Fluorescence spectra in the visible region were determined using a SPEX Fluoromax-2 spectrometer. Near-infrared fluorescence spectra were obtained using a specially equipped Fluoromax-2, kindly made available by Prof. N. A. P. Kane-Maguire at Furman University. Simultaneous cyclic voltammetry and electron paramagnetic resonance were performed using a BAS-100W potentiostat, a three-electrode cell, a rectangular cavity, and a Varian E-12 EPR spectrometer. Langmuir−Blodgett films were obtained using a microcomputer-controlled Nima model 622D2 trough connected to a Lauda constant-temperature bath (5−30 °C), in a room with HEPA-filtered air, and high resistivity water (Millipore Milli-Q, 18 MΩ cm). NMR spectra were observed using a Bruker AM360 NMR spectrometer and DMSO-d_6 as the solvent, in the temperature range 298.15−355 K, taking care that the solution was filtered through a Pasteur pipet to remove any undissolved compound.

X-ray photoelectron spectra (XPS) of LB monolayers and multilayers were obtained using a Kratos Analytical Axis 165 Scanning Auger/X-ray Photoelectron Spectrometer. Monochromatized Al Kα photons ($E = 1486.6$ eV) were used as the exciting radiation, giving an intrinsic spectrometer resolution of <0.2 eV. The spectra were fit using a proprietary program from Kratos Analytical, which applied Lorentz−Gaussian peak shapes and instrument-specific fitting parameters.

Equations for solvatochromism were written using a Digital Visual FORTRAN 5.0 compiler on a IBM Thinkpad 365 XD PC microcomputer. Molecular orbitals were calculated using the CaCHE programming system on a Macintosh PowerPC 8100 microcomputer; a trial geometry was first optimized by molecular mechanics, then minimized again using the PM3 algorithm at the single-determinant restricted Hartree−Fock (RHF) level for the ground state and the first singlet excited state (no solvent models were included).

4. Absorption and Fluorescence Spectra in Solution

The absorption and fluorescence spectra of **1** were measured at room temperature in up to eight solvents. The spectra are

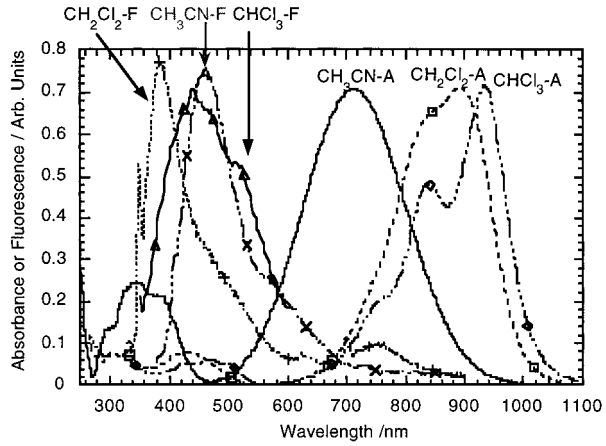

Figure 1. Absorption ($-A$) and fluorescence ($-F$) spectra (exciting wavelength = 300 nm) of solutions of **1** in chloroform ($CHCl_3$), dichloromethane (CH_2Cl_2), and acetonitrile (CH_3CN) at room temperature. A solvent Raman line is seen at 320 nm in CH_2Cl_2.

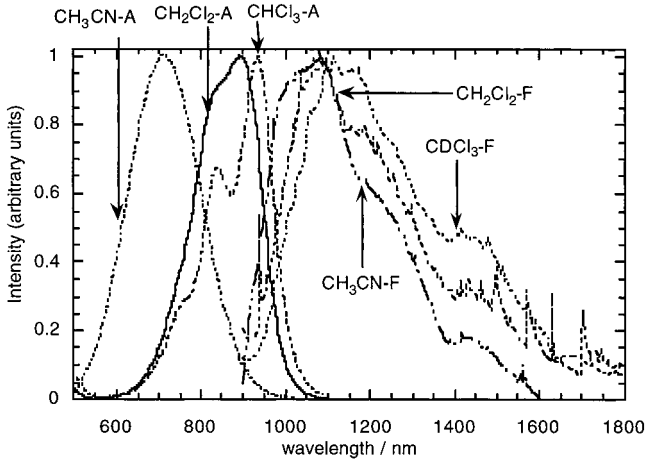

Figure 2. Absorption ($-A$) and fluorescence ($-F$) spectra (exciting wavelength = 350 nm) of solutions of **1** in chloroform ($CHCl_3$)/deuteriochloroform ($CDCl_3$), dichloromethane (CH_2Cl_2), and acetonitrile (CH_3CN) at room temperature.

summarized in Figures 1 and 2, and relevant data are listed in Tables 1 and 2. The long-wavelength absorption bands have two peaks in the lower polarity solvents chloroform, dichloromethane, ethyl acetate, and tetrahydrofuran; these peaks merge into one in acetone, nitromethane, and acetonitrile. The two closely spaced absorption peaks in the lower polarity solvents may be due to rotamers, but more likely are vibronically resolved features.

Although it was determined previously that the low-energy visible absorption maximum of **1** is linear with concentration in CH_3CN and in CH_2Cl_2, and almost linear in $CHCl_3$,[1] i.e., obeys Beer's law, a renewed search was made for a monomer−oligomer equilibrium by measuring the visible−UV spectrum as a function of solution temperature and of concentration; no isosbestic points were found in several solvents as a function of temperature, e.g., in CH_2Cl_2 in the range −5 to 30 °C or in CH_3CN in the range 5 to 50 °C. Therefore, the spectra in Figures 1 and 2 are attributed to the monomer of **1**.

The visible emission band in CH_2Cl_2 (excitation at 300 nm) includes a strong Raman emission at 320 nm. The quantum efficiency ϕ of the visible emission of **1** in CH_2Cl_2 was compared to that of pyrene ($\phi = 0.92$) and was found to be low ($\phi = 0.007$); a rough estimate of ϕ by direct photometric methods gave $\phi \approx 0.01 \pm 0.02$. The near-infrared emission spectra (Figure 2, excitation at 350 nm) were weak and noisy; several spikes due to atmospheric muons were removed from the data.

The short-wavelength absorption maxima (underlined in Table 1) do not vary monotonically with dielectric constant or index of refraction (or other functions combining these). The long-wavelength absorption bands are strongly solvatochromic; they are hypsochromic (Figure 3) and shift almost linearly (blue shift) with dielectric constant (Figure 3). This indicates that the ground state has a higher dipole moment than the electronically excited state. There is only a small "salt effect" in CH_2Cl_2 but not in CH_3CN; when Bu_4NPF_6 is added to a CH_2Cl_2 solution of **1**, the long-wavelength absorption peaks shift from a doublet at 891.5 and 843 nm to a single maximum at 830 nm. Adding Bu_4NPF_6 to an CH_3CN solution of **1** produces no shifts. Increasing the temperature of a $CHCl_3$ solution of **1** from 22 to 58 °C does not produce any shifts in the absorption spectrum.

There are two sets of fluorescent emission lines: emissions below 600 nm and emissions in the 1000−1400 nm region. The emissions in the near-IR region are very weakly hypsochromic. That two fluorescent emissions exist for **1** is an apparent violation of Kasha's rule,[19] which dictates that, within a set of states of the same spin multiplicity, a fluorescent emission should occur only from the lowest excited state. Other, higher excited states usually decay, internally and without radiative emission, into the lowest excited state, which then emits the photon.

However, if the higher energy emission is weak (here $\phi \approx 0.01$) and is not reabsorbed, then emission from a higher energy state becomes possible.[20] Alternatively, molecule **1** may have different rotameric states; molecules of **1** with $\theta \approx 90°$, with no IVT, would emit in the visible, while molecules with a lower θ and a "blue" IVT will emit in the near-infrared region.

Much effort was devoted to estimating the excited-state dipole moment from theories of solvatochromism.[17] An equation, based on Onsager solution theory, introduced by McRae,[21] was modified in minor ways by later authors:

$$[\nu_{gas} - \nu_{soln}]/5.0341 \times 10^3 = [(\mu_g\mu_e \cos\phi - \mu_g^2)/a^3][2(\epsilon - 1)/(2\epsilon + 1) - 2(n^2 - 1)/(2n^2 + 1)] + [(\mu_e^2 - \mu_g^2)/a^3][2(n^2 - 1)/(2n^2 + 1)] \quad (1)$$

This equation links[17] the absorbance maximum in solution ν_{soln} (cm^{-1}), the absorbance maximum in the gas phase ν_{gas} (cm^{-1}), the ground-state dipole moment μ_g (Debyes), the excited-state dipole moment μ_e (Debyes), the angle ϕ between these two dipoles, the solute cavity volume a^3 (Å^3), the dielectric constant ϵ, and the index of refraction n. The first and second terms on the right-hand side describe the spectral shifts due to the dipolar reaction field and the inductive field, respectively.[17] This equation and its minor variations have been used to estimate μ_e and ϕ.[17−25]

An independent estimate of the excited-state dipole moment μ_e can be made by comparing the absorption and fluorescent emission energies, assuming no change in the orientation of the dipole.[26] Adapting eq 1 for absorption and emission, neglecting the generally small inductive field term $[(\mu_e^2 - \mu_g^2)/a^3][2(n^2 - 1)/(2n^2 + 1)]$, assuming that the solvent cavity radius a is the same for absorption as for emission and that the dipole moments in the ground and excited states are collinear, the ratio of the energy shift between any two solvents for absorption ΔE_a and for fluorescence ΔE_f is given by[26]

$$\Delta E_a/\Delta E_f = \mu_g/\mu_e \quad (2)$$

TABLE 1. Absorption and Fluorescent Emission Spectral Maxima (λ_{Max}, Nm) of 1 in Three Solvents and in Solid Films[d]

$CHCl_3$ $\epsilon = 4.810$[a]; $n = 1.4459$[a]		CH_2Cl_2 $\epsilon = 8.93$[a]; $n = 1.4242$[a]		CH_3CN $\epsilon = 37.5$[b]; $n = 1.3441$[a]		1-layer LB film		11-layer LB film[c]	
abs, λ_{max}	emiss	abs, λ_{max}	emiss	abs, λ_{max}	emiss	abs, λ_{max}	emiss	abs, λ_{max}	emiss
		230		227				240s	
265		244		239					
315		303		297					
326		329		345.5		340		337s	
				380	438			383	
440s	462	430	383		467				
469	565s				498				
750s			753						
839		**843**		**711**		**565**	**492**	**570**	
933.5		**891.5**							
838[1]		**884[1]**		**711[1]**	**875**				
	1113*		**1098**		**1080**				

[a] From ref 17. [b] From ref 18. [c] From ref 1. [d] "s" denotes shoulders; the most intense peaks are underlined. The IVT bands are given in boldface. The excitation for the fluorescent bands was at 300 nm. Also listed are the zero-frequency static dielectric constants ϵ at 20 °C[17,18] and the Na−D Line Indices of refraction n.[17] (*) Indicates that the near-IR Fluorescence Was Run in $CDCl_3$.

TABLE 2: Absorption Spectral Maxima (ν_{max}/cm^{-1}) for IVT of 1 in Eight Solvents, with Relevant Dielectric Constants ϵ and Indices of Refraction[a] n

	ν_{max}						
$CHCl_3$	AcOEt	THF	CH_2Cl_2	pyridine	CH_3COCH_3	CH_3NO_2	CH_3CN
$\epsilon = 4.810$	6.02	7.58	8.93	12.91	20.56	35.94	37.5
$n = 1.4459$	1.3724	1.4072	1.4242	1.5102	1.3724	1.3819	1.3441
11920	12030	11930	11860	12300	13000	13970	14060
10710	11920	11140	11220				
[8993]	[8702]	[8734]	[8002]	[8607]	[8407]	[8992]	[8890]

[a] In [square brackets] are given the estimates of $E(\upsilon)$ (cm^{-1}), using eqs 2, 5, 6, and 7 and the following data. The cavity semimajor axis is A = 10.5 Å; the semiminor axis is 3.449 Å; the reciprocal ellipticity is 1.05875. The molecular dielectric constant is $\epsilon_m = 2.0$. The N atom position is at Cartesian angstrom coordinates (0, 0, −0.20 Å) and prolate spheroidal coordinates (0, 0, −0.20/A). The C atom is at Cartesian angstrom coordinates (0, 0, 10.20 Å) and prolate spheroidal coordinates (0, 0, 10.20/*A*). The ground-state charges are $\zeta_C = -1.0$ and $\zeta_N = 1.0$ for C and N, respectively. The excited-state charges are $\zeta_C^* = -0.2$ and $\zeta_N^* = 0.2$. For the four solvents where two close IVT absorption maxima are observed, the higher energy maximum (first line) was used in the calculation. The average of the eight calculated $E(\upsilon)$ values is $\langle E(\upsilon)\rangle = 8665 \pm 312$ cm^{-1}.

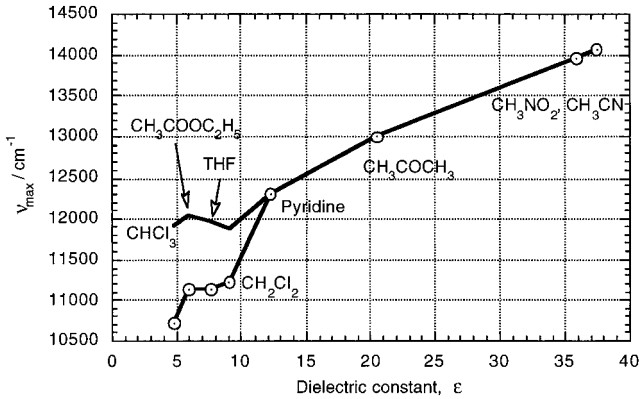

Figure 3. Hypsochromic (blue) shift of long-wavelength absorption maxima with increasing dielectric constant of the solvent.

The data of Table 1 are, for the IVT band, $E_a = 11920$ cm^{-1} and $E_f = 8985$ cm^{-1} for $CHCl_3/CDCl_3$, $E_a = 11860$ cm^{-1} and $E_f = 9108$ cm^{-1} for CH_2Cl_2, and finally $E_a = 14060$ cm^{-1} and $E_f = 9260$ cm^{-1} for CH_2Cl_2. Using $\mu_g = 43$ D[1] and eq 2, these data yield $\mu_e = 5.53$ D ($CHCl_3$ − CH_3CN) or $\mu_e = 2.97$ D (CH_2Cl_2 − CH_3CN).

Using the data of Table 2 and several variants of eq 1 provided no reasonable estimate of μ_e and ϕ. An explanation was found in a thorough discussion of solvatochromism[27] all equations similar to eq 1 assume point dipoles. When the charge separation is of the same magnitude as the size of the cavity, then such equations fail. The analysis by Kirkwood and Westheimer[28,29] has been updated to provide a more general treatment of the problem.[27] The shift from the absorption maximum $E(\text{abs},\epsilon)$, in a solvent of dielectric constant ϵ and refractive index n, to the excitation energy in a vacuum, $E(\upsilon)$, is given by the energy difference[27]

$$E(\text{v}) - E(\text{abs},\epsilon) = w(\zeta^*,\epsilon) - w(\zeta,\epsilon) + w(\zeta^*-\zeta,n^2) - w(\zeta^*-\zeta,n^2) \quad (3)$$

where $w(\zeta, \epsilon)$ is the reversible work of charging a molecule from zero to a charge distribution ζ (in the ground state) or ζ^* (in the excited state), when embedded in a cavity surrounded by a solvent of dielectric constant ϵ.[27] The work for a molecule of dielectric constant ϵ_m placed in a spherical cavity of radius a becomes.[27]

$$w(\zeta,\epsilon) = (q^2/2a)(\epsilon^{-1} - 1) - (1/2a)\{(\epsilon_m{}^{-1} - \epsilon^{-1})\sum_n g_n[1 + \epsilon_m n/\epsilon(n+1)] - (\epsilon_m{}^{-1} - 1)\sum_n g_n[1 + n/\epsilon(n+1)]\} \quad (4)$$

where both sums over n extend from $n = 1$ to infinity, and g_n is given by

$$g_n = \Sigma_j\Sigma_k\zeta_j\zeta_k(r_j/a)^n(r_k/a)^n P_n(\cos\theta_{jk}) \quad (5)$$

where the double sum over j, k extends over all atoms in the molecule. These atoms j, k have fractional point charges ζ_j, ζ_k and distances r_j, r_k from the center of the sphere, respectively. $P_n(\cos\theta_{jk})$ is the n-th Legendre polynomial of the first kind with argument $\cos\theta_{jk}$, and θ_{jk} is the angle between vectors r_j

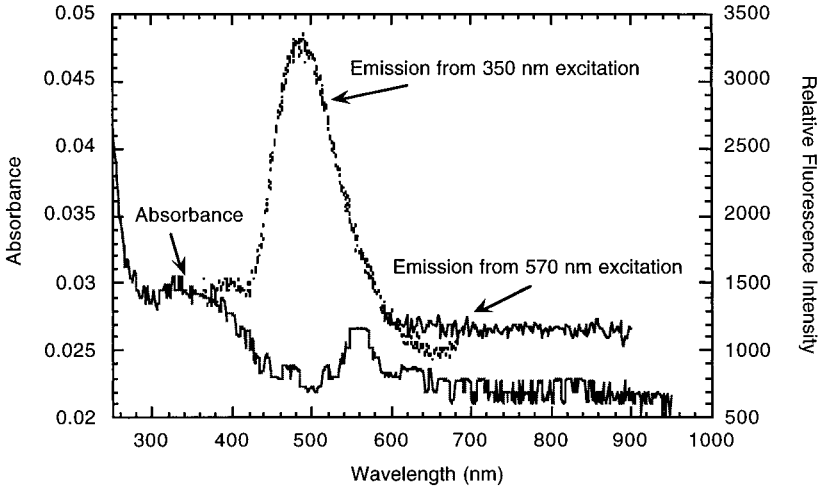

Figure 4. Visible absorption and emission spectrum of a one-monolayer LB film of **1** on quartz. The lower curve is the absorbance (maxima at 340 and 565 nm); the upper curve is the fluorescence emission, which peaks at 492 nm (for excitation at 350 nm). The short curve on the right is the fluorescence emission (for excitation at 570 nm, i.e., at the maximum of the absorbance).

and r_k. The first term of eq 4, the Born charging term, where q is the total charge of the molecule, usually vanishes.

Equations 3, 4, and 5 were programmed in FORTRAN, and tried, but with limited success. Molecule **1**, with a long molecule of total length 20−30 Å, depending on conformation, when approximated with unit point charges localized at the quinolinium N atom and at the apical C atom of the dicyanomethylene end (which are separated by about 10 Å[1]), provided shifts $E(\upsilon) - E(\text{abs}, \epsilon)$ that were too small and varied greatly with the solvent; a spherical cavity was not appropriate for **1**.

Since **1** is a large and long molecule, with an asymmetrical distribution of charge, a prolate spheroidal cavity model seemed more apt. Fortunately, the equivalent of eq 4 is available for atoms placed along the major axis of a prolate spheroidal cavity.[28,29] This restriction is adequate for the present purpose. When the molecule is in a prolate spheroidal cavity and consists of charged atoms along the major axis, then eqs 4 and 5 become[29]

$$w(\zeta,\epsilon) = (1/R)\,(\epsilon_{\text{m}}{}^{-1} - \epsilon^{-1}) \sum_n X_n/I_n(\epsilon_{\text{m}},\epsilon) \qquad (6)$$

where R is the interfocal length, and

$$X_n = 2(2n+1)\{1-(-1)^n\} \sum_j \sum_k \zeta_j\zeta_k P_n(z_j)P_n(z_k)Q_n(\lambda)/\text{P}_n(\lambda) \qquad (7)$$

$$I_n(\epsilon_{\text{m}},\epsilon) = 1 - \epsilon_{\text{m}}[\lambda - P_{n+1}(\lambda)/P_n(\lambda)]/\epsilon[\lambda - Q_{n+1}(\lambda)/Q_n(\lambda)] \qquad (8)$$

where atoms are placed at positions $r_k = Rz_k$ along the major axis. λ is the reciprocal ellipticity $\lambda = A(A^2 - B^2)^{-1/2}$, where A and B are the semimajor and semiminor axes, respectively. $Q_n(\lambda)$ is the Legendre polynomial of the second kind of order n and argument λ, and $P_n(x)$ is again the n-th Legendre polynomial of the first kind with argument x. Equations 6−8 were added to the computer program, using a FORTRAN algorithm for Q functions of argument larger than 1.[30] The calculated values of $E(\upsilon)$ are included in Table 2. The narrow spread in the calculated values of the energy difference between ground and first excited state in a vacuum, combined with reasonable values for the cavity dimensions, suggest that the calculation was successful. The resultant estimate of the excited-state dipole moment is a very reasonable $4.184 \times 0.2 \times 10.4 = 8.7$ D.[31]

5. Absorbance and Emission of a LB Monolayer

An LB monolayer of **1**, transferred onto quartz, shows weak absorption maxima at 340 nm and at 565 nm (Figure 4). The same monolayer, excited at 350 nm, produces a clear emission peak at 492 nm, but no emission when excited at 570 nm. Previously, an 11-layer LB film showed absorbances at 240 (shoulder), 337(shoulder), 383, and 565 nm.[1] The absorption of a solid film of 15 Langmuir−Blodgett monolayers of **1** on quartz was checked visually for changes between room temperature and 77 K; the films are blue-violet at both temperatures, thus arguing for no large change in the twist angle θ between these two temperatures.

6. NMR Spectrum as a Function of Temperature

The proton NMR spectrum of **4** in DMSO-d_6 has the following resonances at 298 K: δ 9.38 (d, 1H, H-2, $J = 5.80$ Hz, int=0.98), 8.72 (d, 1H, H-8, $J = 8.50$ Hz, int=0.93), 8.47 (d, 1H, H-5, $J = 8.96$ Hz), 8.46 (d, 1H, H-3, $J = 6.35$ Hz), 8.45 (s, 1H, H-11) (for H-5, H-3, and H-11, int = 2.72), 8.24 (t, 1H, H-6, $J = 7.86$ Hz, int = 0.98), 8.04 (t, 1H, H-7, $J = 7.72$ Hz, int = 0.100), 7.74 (d, 2H, H-13, $J = 8.27$ Hz, int = 1.91), 6.90 (d, 2H, H-12, $J = 8.59$ Hz, int = 1.83), 4.55 (t, 3H, $J = 7.16$ Hz, int = 2.81).

The NMR spectrum broadens above 330 K; above 345 K, the multiplets cannot be resolved. As shown in Figure 5, three signals shift downfield with increasing temperature (decreasing $1/T$): the singlet due to H-3 from δ 8.45 at 298 K to δ 8.34 at 340 K; the doublet due to H-2 from δ 9.38 at 298 K to δ 9.28 at 350 K, and the doublet due to H-13 from δ 7.74 at 298 K to δ 7.68 at 350 K. These shifts are consistent with a larger contribution to the ground state of the less polar conjugated conformer **1′** (i.e., decrease in the twist angle θ) at higher temperatures. The collapse of the multiplets at 345 K may be due to increased intramolecular motion, with rapid exchange between states.

7. Electron Paramagnetic Resonance Spectrum of the Radical Anion of 1

A saturated solution of **1** in dimethylformamide (DMF), with 0.1 M Bu_4NPF_6 electrolyte added, was bubbled with Ar at room temperature and introduced into the electrochemical EPR cell at room temperature under an Ar atmosphere. The electrode

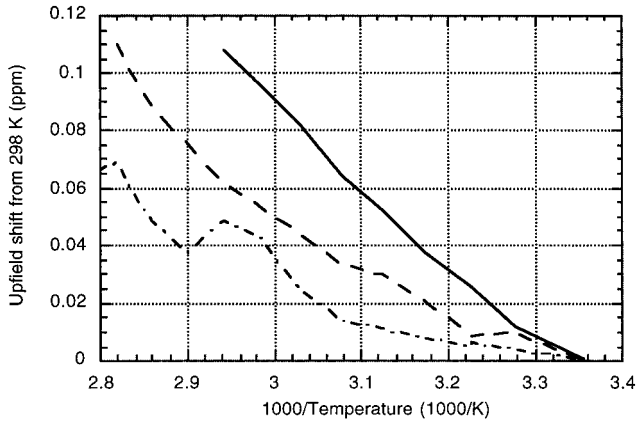

Figure 5. Upfield shifts with increasing temperature of the NMR resonances δ (ppm) for H-2 (dashed line), H-3 (solid line), and H-15 (dot−dashed line) of molecule **4** in DMSO-d_6.

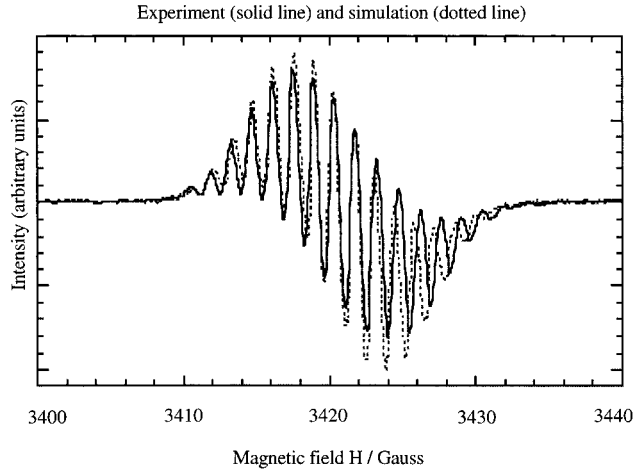

Figure 6. Electron paramagnetic resonance spectrum of the radical anion of **1**, electrogenerated in DMF at −0.645 V vs SCE, with 0.1 M Bu_4NPF_6. The simulated spectrum is shown as dashed lines.

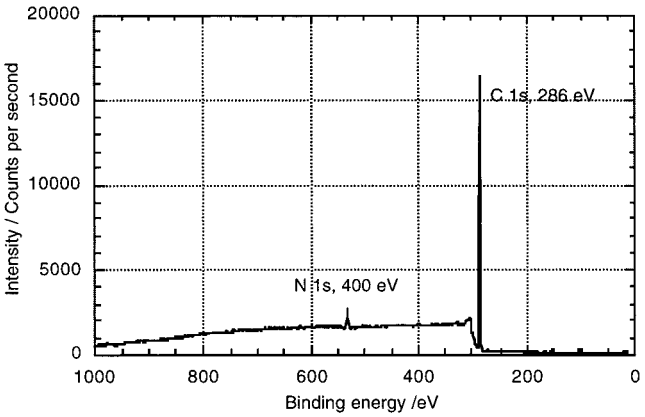

Figure 7. Wide-scan X-ray photoelectron spectrum of an LB multilayer on Si.

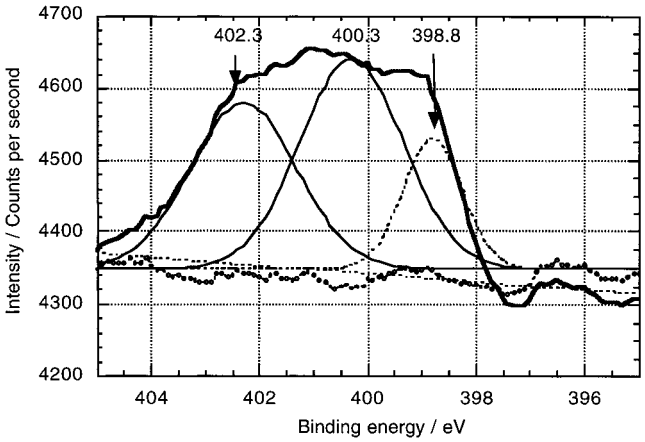

Figure 8. Nitrogen N 1s region of the X-ray photoelectron spectrum of an LB multilayer of **1** on Si. Also shown are a sloping linear background fit, Gaussian peak fits to simulate the spectrum, and the error in the fit (small circles). N 1s peaks are seen at 402.3, 400.3, and 398.8 eV.

potential was held 0.1 V more negative than the first reduction peak potential of **1** (−0.645 V vs SCE). The EPR spectrum was recorded at 9.5866 GHz (Figure 6), then simulated (Figure 9)[32] using $g = 2.0027$ and isotropic hyperfine constants $a_N =$ 1.20 G ($2 \times {}^{14}N$, $I = 1$) and 2.80 G (^{14}N), $a_H = 1.44$ G ($2 \times {}^{1}H$, $I = 1/2$), 1.80 G ($2 \times {}^{1}H$), and 3.0 G (^{1}H). The coupling constants on the four 3CNQ ring protons and the two cyano nitrogens are very close to the data for the radical anion of TCNQ ($a_N = 1.02$, $a_H = 1.44$ G)[22] and thus testify that most of the spin density in the radical anion of **1** is localized on the 3CNQ part of the molecule and the bridgehead proton, as shown in structure **1**‴.

8. N 1s Core-Level X-ray Photoelectron Spectrum of Langmuir−Blodgett Films

Figure 7 shows the XPS spectrum of an LB multilayer of **1** adsorbed on an oxide-covered Si substrate. The only features are for C (1s, 286 eV) and N (1s, ∼400 eV).

Figure 8 shows the N 1s region in detail. The feature associated with nitrogen is clearly composed of three peaks, which have been fit using standard techniques. The dominant feature at 400.5 eV is in the range for N in an organic matrix (398.9−401.0 eV[33]), exactly what one would expect from this molecule, given its chemical formula. However, there are features at higher (402.3 eV) and lower (398.8 eV) binding energies, which indicate the charge transfer state of the molecule. The lowest energy feature (398.8 eV) can be associated with nitrogen in the C≡N moiety of ionic salts such as KCN (N 1s 398.3−399.8 eV[34]). The highest binding energy feature (402.3 eV) is in the range associated with ammonium salts, e.g., $N^*H_4NO_3$ at 402.3 eV.[35] The shift to lower binding energy reflects reduction or the increase in local electron density, and the shift to higher binding energy reflects oxidation or a decrease in local electron density. These results are totally consistent with the depiction of **1** which shows internal charge transfer.

There is evidence that the soft X-rays degrade the thin organic film over time. Spectra of the Langmuir−Blodgett monolayer (not shown), prepared in exactly the same way as the multilayers described above, do not show such strong separation of features in the N 1s region.

Instead, the N peak is centered at 400.3 eV and represents an undifferentiated N signal from an organic layer. Degradation of the films may also explain why the peak fit integrated areas do not scale with the ratio of different N atoms in **1**. One would expect a ratio of 1:1:2 for the features assigned to 402.3, 400.3, and 398.8 eV, respectively, in Figure 8. It appears that either the X-ray photons or the passage of time (or both) degrades the sample, leaving more of the undifferentiated nitrogen feature than would be expected.

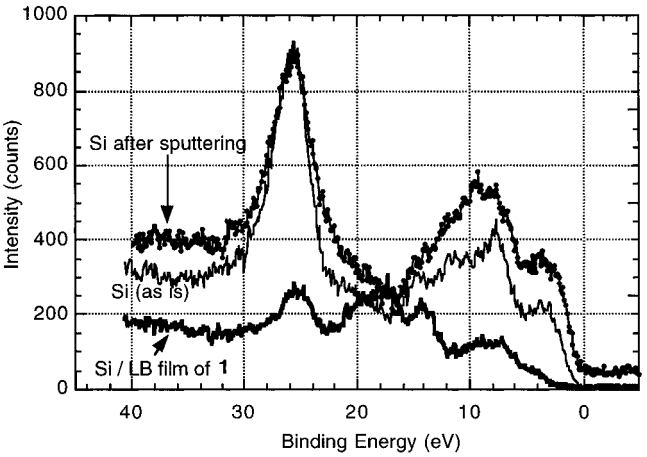

Figure 9. Valence-band XPS spectrum of an LB multilayer of **1** on Si (lowest scan), of the highly degenerate Si substrate as received, and of the Si substrate after Ar^+ sputtering (top scan).

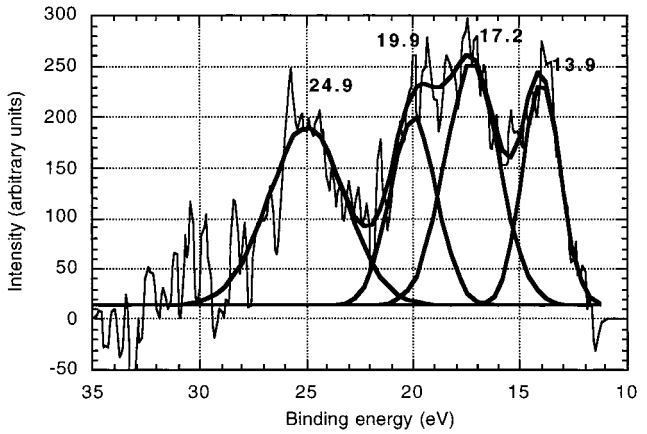

Figure 10. Valence-band XPS spectrum of an LB multilayer of **1** on Au (difference between LB film and Au substrate) with Gaussian line fits.

9. Valence Band X-ray Photoelectron Spectrum of Langmuir−Blodgett Films

A valence band scan of a multilayer of **1** on Si (Figures 9, 11) and on Au (Figure 10) reveal several peaks at binding energies of 3−25 eV. Strong signals from the Au substrate in the 3−8 eV range (not shown) are much attenuated when the LB film covers it, but the signals from the LB film may still be Au signals, rather than LB film features, so this region of the spectrum is not shown in Figure 10. For Si there are features in the 2−6 eV binding energy range, which do not diminish after Ar^+ sputtering, but they are weaker, so the valence band spectrum for the LB film is shown in full in Figure 11. A fit with Gaussian peaks was performed; the binding energies of the centers of these Gaussians are reported in Figures 10 and 11. There is strong agreement between the LB film peaks seen on Au and those seen on Si.

To compare with theory the valence-band XPS spectral peaks, Table 3 shows these experimental peaks adjusted to the vacuum level ($E = 0$) by adding to the binding energies the work functions (≈Fermi levels) of 4.1 eV[18] for Si and 4.58 eV for Au and changing the sign. These values are then compared in Table 3 with a geometry-optimized PM3/RHF semiempirical molecular orbital calculation of the ground state of **1**. Where the data exist, there is strong agreement between theory and experiment. The fit between the onset of the valence-band XPS at 3.7 eV on Si (−7.8 eV versus *E*(vacuum)) and the calculated

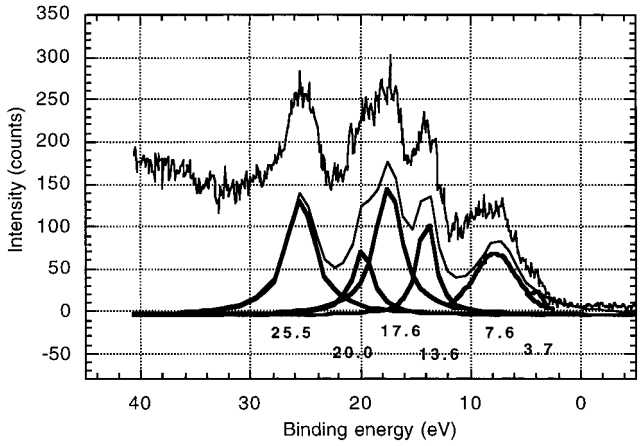

Figure 11. Valence-band XPS spectrum of an LB multilayer of **1** on Si with Gaussian line fits.

HOMO at −7.98 eV is remarkable. The experimental XPS spectra can be resolved into four to six broad peaks (Figures 10 and 11), while the PM3 calculation has 107 closely spaced occupied molecular orbitals (Figure 12). The escape probabilities from each MO would have to be computed to improve the fit.

However, the same calculation for the ground state of **1** obtains a dipole moment of only 10.7 D. A PM3/RHF calculation for the excited singlet (dihedral angle θ close to 90°) does not agree well, although it yields a large moment of 45.4 D.

10. Discussion

The long-wavelength absorptions are clearly hypsochromic; they are associated with a large reduction in dipole moment between ground and excited state. It is clear that the ground state is more ionic than the excited state, in agreement with the assigment of a zwitterionic structure to the ground state.[1] The fluorescent emission bands in the range 350−550 nm are not solvatochromic, because they originate from absorption and emission bands that involve only parts of the molecule. Solvatochromism is expected, and found, for those optical IVT transitions, between 550 and 1000 nm, which involve overall the whole molecule. The excited-state dipole moment is estimated as 8.7 D, whereas the ground-state moment was measured as 43 ± 8 D.[1] Given that the same IVT transition exists both in monolayer and multilayer films ($\lambda_{max} = 565$ nm) and in solution ($\lambda_{max} = 839$ nm in $CHCl_3$ to 711 nm in CH_3CN), it is difficult to agree with the theoretical supposition[11,12] that the ground state is much less polar in films than in solution. The estimated vacuum IVT transition at about 8700 cm^{-1} is lower than the IVT transition observed at 17 700 cm^{-1} in monolayer and multilayer films, but in a zwitterionic film extensive dielectric screening will stabilize the ground state and increase the energy of the IVT transition. For a single crystal of the related molecule **2**, with even more screening, the IVT was found at 18 600 cm^{-1}.[8] There is no spectral evidence for a monomer−dimer or monomer−oligomer equilibrium in solution.

The fluorescent emission in the region 500−900 nm is weak ($\phi \approx 0.01$); the quantum efficiency of the NIR emission was not measured. The dual fluorescence emission suggests either that the relatively weak higher energy emission is not reabsorbed or that there may be at least two rotamers for **1**, one colorless (with no IVT, fluorescence emission in the visible, and ground state $\theta = 90°$) and one colored (with IVT, near-IR fluorescent emission, and ground state $\theta = 30-50°$).

TABLE 3: Molecular Orbital Energy Levels for 1 (eV; $E = 0$ at vacuum level): Experimental (Valence Band XPS) and Theoretical (PM3/RHF)[a]

exptl XPS on Si ($-E_{VB-XPS}$ −4.1) (Figure 10)	exptl XPS on Au ($-E_{VB-XPS}$ −4.58) (Figure 11)	ground-state singlet PM3/RHF calcd ($\Delta H_f = +6.02$ eV) $\mu = 10.7$ D	excited singlet PM3/RHF calcd ($\Delta H_f = +8.47$ eV) (Figure 10)
−29.6	−29.5	−29.8 (#15)	
−24.1	−24.5	−24.1 (#22)	
−21.7	−21.8	−21.7 (#29)	
−17.7	−18.5	−17.8 (#41)	
−11.7		−10.53 (#103)	−10.00 (#103)
		−10.09 (#104)	−9.99 (#104)
		−9.09 (#105)	−9.34 (#105)
−7.8		−7.9 (#106:HOMO)	−5.70 (#106:1e)
		−2.42 (#107:LUMO)	−3.92 (#107:1e)
			−1.16 (#108)

[a] The valence band XPS Energy Levels (E_{VB-XPS}) were corrected to the vacuum level by adding the work functions of Au (4.58 eV[18]) and Si (4.1 eV[18]) and changing the signs. The fit of the XPS spectrum with the excited singlet levels is poor. For the ground-state singlet calculation there are 7 calculated MO's in the energy range −31.0 to −28.0 EV, 3 in the range −25.0 to −23.0 eV, 11 in the range −22.0 to −20.0 eV, and 13 in the range −19.0 to −16.0 eV(Figure 12).This paper needs a title running head (TRH).

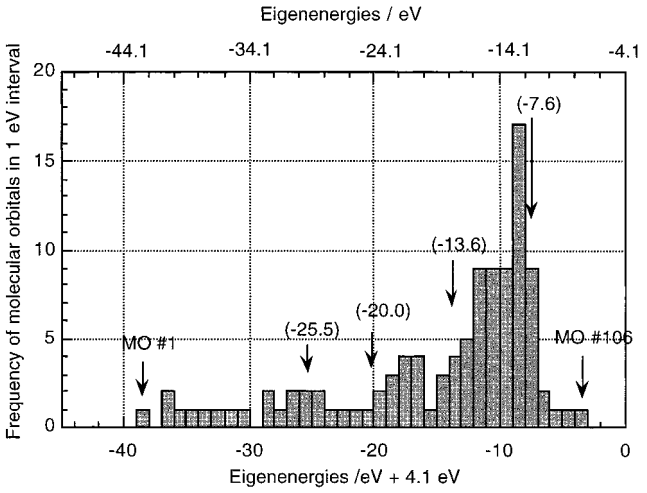

Figure 12. Histogram of occupied molecular orbitals, from PM3/RHF calculation of the ground state of **1**. The bottom abscissa axis gives the eigenvalues, shifted by 4.1 eV for better comparison with Figure 11; the numbers in parentheses show the XPS peaks from Figure 11. The upper abscissa axis gives the eigenvalues relative to the vacuum level (same as in the third column of Table 3).

The temperature-dependent NMR spectrum shows a broadening at 330 K and collapse of multiplet structure above 345 K.

The core-level XPS spectrum confirms several valences for N in the molecule; the valence-band XPS spectra can be correlated very well with the calculated PM3 (AM1) occupied molecular orbitals. However, the calculated PM3 dipole moments remain a problem.[1] The charge separation in zwitterions is not well reproduced by PM3 or other similar semiempirical molecular orbital theories; this problem is well-known,[3,10] but it may transcend "solvent effects" and result from some "weakness" in the approximate molecular Hamiltonian.

The spin distribution seen by EPR is consistent with a radical, whose spin densities are significant only on part of the $3CNQ^-$ species. Previous MO calculations on **1** indicate[1] that the LUMO of **1** should be mostly localized on the $3CNQ^-$ part of the molecule, in agreement with observation.

11. Conclusion

We have proven that the excited-state dipole moment of $C_{16}H_{33}Q$-3CNQ is much smaller than its ground-state moment and confirmed its zwitterionic ground state by N 1s core-level XPS spectra. The occupied molecular orbitals have been estimated by valence-level XPS; in the electron spin resonance spectrum of the radical anion of $C_{16}H_{33}Q-3CNQ$, the spin density is confined on the 3CNQ end of the molecule.

Acknowledgment. We are grateful to the National Science Foundation (DMR-94-20699) and to the Department of Energy (DOE-EPSCoR DE-FC02-91-ER-75678) for support, to the National Science Foundation (DMR-95-12264) for the acquisition of the XPS spectrometer, and to Prof. N. A. P. Kane-Maguire (Furman University) for the use of his NIR fluorometer. One of us (C.S.S.) thanks the DOE-EPSCoR program for Minority Summer Research support.

References and Notes

(1) Metzger, R. M.; Chen, B.; Höpfner, U.; Lakshmikantham, M. V.; Vuillaume, D.; Kawai, T.; Wu, X.; Tachibana, H.; Hughes, T. V.; Sakurai, H.; Baldwin, J. W.; Hosch, C.; Cava, M. P.; Brehmer, L.; Ashwell, G. J. *J. Am. Chem. Soc.* **1997**, *119*, 10455−10466.

(2) Aviram, A.; Ratner, M. A. *Chem. Phys. Lett.* **1974**, *29*, 277−283.

(3) Broo, A.; Zerner, M. C. *Chem. Phys.* **1996**, *196*, 423−426.

(4) Metzger, R. M.; Heimer, N. E.; Ashwell, G. J. *Mol. Cryst. Liq. Cryst.* **1984**, *107*, 133−149.

(5) Ashwell, G. J.; Sambles, J. R.; Martin, A. S.; Parker, W. G.; Szablewski, M. *J. Chem. Soc., Chem. Commun.* **1990**, 1374−1376.

(6) McKusick, B. C.; Heckert, R. E.; Cairns, T. L.; Coffman, D. D.; Mower, H. F. *J. Am. Chem. Soc.* **1958**, *80*, 2806−2815.

(7) Sandman, D. J.; Richter, A. F. *J. Am. Chem. Soc.* **1979**, *101*, 7079−7080.

(8) Akhtar, S.; Tanaka, J.; Metzger, R. M.; Ashwell, G. J. *Mol. Cryst. Liq. Cryst.* **1986**, *139*, 353−364.

(9) Ashwell, G. J.; Szablewski, M.; Kuczynski, A. P. In *Lower-Dimensional Systems and Molecular Electronics*;, Metzger, R. M., Day, P., Papavassiliou, G. C., Eds.; NATO ASI Series B248; Plenum: New York, 1990; p 647.

(10) Klamt, A.; Schüürmann, G. *J. Chem. Soc., Perkin Trans. 2* **1993**, *5*, 799−804.

(11) Pickholz, M. A.; Dos Santos, M. C. *Synth. Metals* **1997**, *85*, 1775−1776.

(12) Pickholz, M.; Dos Santos, M. C. *J. Mol. Structure (THEOCHEM)* **1998**, *432*, 89−96.

(13) Ashwell, G. J. Private communication.

(14) Lakshmikantham, M. V. Unpublished results.

(15) Ashwell, G. J. In *Organic Materials for Nonlinear Optics*; Ashwell, G. J., Bloor, D., Eds.; Royal Society of Chemistry Cambridge, 1993; pp 31−39.

(16) Martin, A. S.; Sambles, J. R.; Ashwell, G. J. *Phys. Rev. Lett.* **1993**, *70*, 218−221.

(17) Reichardt, C. *Solvents and Solvent Effects in Organic Chemistry*, 2nd ed.; VCH: Weinheim, Germany, 1988.

(18) *American Institute of Physics Handbook*, 2nd ed.; Gray, D. E., Ed.; McGraw-Hill: New York, 1963; p 5−123.

(19) Kasha, M. *Discuss. Faraday Soc.* **1950**, *9*, 14−19.

(20) Geldof, P. A.; Rettschnick, R. P. H.; Hoytink, G. J. *Chem. Phys. Lett.* **1969**, *4*, 59−61.

(21) McRae, E. G. *J. Phys. Chem.* **1957**, *61*, 562.
(22) Fisher, P. H. H.; McDowell, C. A. *J. Am. Chem. Soc.* **1965**, *85*, 2694.
(23) Suppan, P.; Tsiamis, C. *Spectrochim. Acta* **1980**, *36A*, 971−974.
(24) Prabhumirashi, L. S.; Narayanan Kutty, D. K.; Bhide, A. S. *Spectrochim. Acta* **1983**, *39A*, 663−668.
(25) Ledger, M. B.; Suppan, P. *Spectrochim. Acta* **1967**, *23A*, 641−653.
(26) Suppan, P. *Chem. Phys. Lett.* **1983**, *94*, 272−275.
(27) Brunschwig, B. S.; Ehrenson, S.; Sutin, N. *J. Phys. Chem.* **1987**, *91*, 4714−4723.
(28) Westheimer, F. H.; Kirkwood, J. G. *J. Chem. Phys.* **1938**, *6*, 513−517.
(29) Brunschwig, B. S.; Ehrenson, S.; Sutin, N. *J. Phys. Chem.* **1986**, *90*, 3657−3668.
(30) Zhang, S.; Jin, J. *Computation of Special Functions*; Wiley: New York, 1996.
(31) A referee kindly suggested that if in eq 1 the indices of refraction are the same from solvent to solvent, if $\cos\phi = 1$, and if $a^3 = 0.7346(\mathrm{MM}/d)^{1/3}$ [Karelson, M. M.; Zerner, M. C. *J. Phys. Chem.* **1992**, *96*, 6949−6957. MM = molar mass = 544 for **1**, and d = density = 1 for **1**], then for the spectral shift ΔE from $CHCl_3$ to CH_3CN eq 1 becomes $\Delta E = 2140\ \mathrm{cm}^{-1} = (12699/\mathrm{MM})[2(\epsilon_1 - 1)/(2\epsilon_1 + 1) - 2(\epsilon_2 - 1)/(2\epsilon_2 + 1)]43(43 - \mu_e)$, whence $\mu_e = 34$ D. This μ_e is much larger than the estimates provided in the text, yet it is still smaller than μ_g, as required by the discussion. The severe approximations outlined in this note make us prefer the smaller values for μ_e (5.53 or 2.97 or, most likely, 8.7 D) obtained in the text.
(32) Shubin, A. *ESR1* (PC computer program for ESR simulation); Russian Academy of Sciences: Novosibirsk.
(33) *Handbook of X-ray Photoelectron Spectroscopy*; Chastain, J., King, R. C., Eds.; Physical Electronics, Inc.: Eden Prarie, MN, 1985.
(34) Vannerberg, N. G. *Chem. Scr.* **1976**, *9*, 122.
(35) Burger, K.; Tschismarov, F.; Ebel, H. *J. Electron Spectrosc. Relat. Phenom.* **1977**, *10*, 461.